Solvent-dependent ultrafast internal conversion dynamics of n'-apo-β-carotenoic-n'-acids (n = 8, 10, 12)

Sebastian Stalke,[a] Duncan A. Wild,[a] Thomas Lenzer,*[a] Matthäus Kopczynski,[b] Peter W. Lohse[b] and Kawon Oum*[b]

Received 2nd January 2008, Accepted 28th January 2008
First published as an Advance Article on the web 25th February 2008
DOI: 10.1039/b720037d

The ultrafast internal conversion dynamics of 12′-apo-β-carotenoic-12′-acid (12′CA), 10′-apo-β-carotenoic-10′-acid (10′CA) and 8′-apo-β-carotenoic-8′-acid (8′CA) have been investigated by femtosecond pump–probe spectroscopy. The three apocarotenoic acids were excited to the S_2 state with different excess energies. Time constants τ_1 for the IC process S_1/ICT → S_0 were measured by probing the dynamics at 390 nm (S_0 → S_2), 575 nm (S_1/ICT → S_n), 850, 860 and 890 nm (S_2 → S_n and S_1/ICT → S_0). In nonpolar solvents, the observed reduction of the τ_1 values with increasing conjugation length of the acids is consistent with a reduction of the energy gap between the S_1/ICT and S_0 states. The values are in good agreement with those of the corresponding apocarotenals studied previously in our groups. In polar solvents, a pronounced reduction of τ_1 values was observed for 12′CA, however the behavior was different from that observed for the respective aldehyde 12′-apo-β-caroten-12′-al studied previously: First, the degree of τ_1 reduction in methanol was milder for 12′CA (218 → 55 ps) than for 12′-apo-β-caroten-12′-al (220 → 8 ps). Secondly, for 12′CA the plateau of solvent independent τ_1 values extended further into the mid-polar range (up to 0.5 on the Δf scale) than previously observed for the 12′-aldehyde. For 10′CA the polarity effect on the τ_1 values was weaker (~71 ps in *n*-hexane and 34 ps in methanol) and for 8′CA it disappeared completely (~24 ps averaged over all solvents). The polarity-induced reduction of τ_1 is likely due to the stabilization of an intramolecular charge transfer state in polar solvents. This S_1/ICT state is also responsible for the stimulated emission in the near IR, which has been observed in this specific class of carotenoids with a terminal carboxyl group for the first time. The occurrence of stimulated emission in the near IR region is also consistent with the steady-state fluorescence spectra which are reported along with the absorption spectra of these species. Possible reasons for the different behavior of the apocarotenoic acids compared to the respective aldehydes are discussed.

1. Introduction

The unique photophysics and time-resolved dynamics of carbonyl-substituted carotenoids have recently attracted considerable attention.[1–7] In particularly, the intramolecular dynamics of peridinin after excitation to the second electronically excited state S_2 has been in the focus of several ultrafast pump–probe spectroscopic studies, as this molecule is of central importance for the function of the peridinin–chlorophyll a-protein (PCP) complex. A unique feature of peridinin is the strong dependence of the lifetime of its lowest electronically excited state (161 ps in *n*-hexane, 12 ps in methanol),[8,9] which is thought to be due to the presence of a strongly polarity-sensitive state with intramolecular charge transfer (ICT) character.[8–11] The situation is in contrast to carotenoids without carbonyl substitution, like β-carotene. After extensive debates in the literature, which favored either a simple three-state (S_2 → S_1 → S_0) model[12–14] or the involvement of additional excited states in the vicinity of S_2 and S_1,[15,16] a simple three-state relaxation scheme is highly likely for β-carotene[17] on the basis of pump–supercontinuum probe (PSCP) transient absorption spectroscopy[18,19] covering a wide spectral window (330−1000 nm) at high temporal resolution (~10 fs), see ref. 17 and the accompanying extensive supporting information.

For carbonyl carotenoids the nature of the ICT contributions is still under debate. The transient dynamics of peridinin's excited state absorption band in the 500–700 nm region have been interpreted in terms of the presence of two separate yet closely coupled states (S_1 and ICT).[2,20] It is however not clear, whether one or two states are responsible for the observed behavior,[7] and different interpretations have been suggested.[2,11,20–22] Typically, the appearance of ICT character is signaled by the emergence of an additional transient stimulated emission feature in the near IR region, which decays with a time constant similar to that of the excited state absorption in the visible. Until very recently, evidence for ICT character

[a] *Max-Planck-Institut für biophysikalische Chemie, Abt. Spektroskopie und Photochemische Kinetik (10100), Am Fassberg 11, D-37077 Göttingen, Germany. E-mail: tlenzer@gwdg.de; Fax: 49 551 2011501; Tel: 49 551 2011344*
[b] *Georg-August-Universität Göttingen, Institut für Physikalische Chemie, Tammannstrasse 6, D-37077 Göttingen, Germany. E-mail: koum@gwdg.de; Fax: 49 551 393150; Tel: 49 551 3912598*

in carbonyl carotenoids was found only in polar environments.[10] However, in our time-resolved studies on 12′-apo-β-caroten-12′-al and 8′-apo-β-caroten-8′-al stimulated emission was also clearly detected in solvents like *n*-hexane or *i*-octane.[7] Obviously, ICT character in carbonyl carotenoids can also be present in the excited state dynamics in nonpolar environments.

To fully understand the intramolecular dynamics of C=O substituted carotenoids, it is necessary to investigate a wide range of species with varying types of substituents (−CO−R) at different positions of the conjugated chain and with varying conjugation length in nonpolar and polar environments. Along this line, we have studied the three aldehyde substituted apocarotenals 4′-apo-β-caroten-4′-al, 8′-apo-β-caroten-8′-al and 12′-apo-β-caroten-12′-al.[5–7] The behavior of the 12′-species was particularly remarkable, as it showed a very strong reduction of the lifetime of the first electronically excited state with increasing solvent polarity (∼220 ps in *n*-hexane, ∼8 ps in methanol), due to the presence of ICT character, which results in a stronger relative stabilization of the excited state compared to the electronic ground state. An interpretation in the framework of an energy-gap-law type approach would then suggest a faster nonradiative transition back to S_0.[23,24]

In the present work, we extend our studies to the carboxyl substituted species 8′-apo-β-carotenoic-8′-acid (8′CA), 10′-apo-β-carotenoic-10′-acid (10′CA) and 12′-apo-β-carotenoic-12′-acid (12′CA). Fig. 1 illustrates their chemical structures. There are two previous experimental investigations available, which deal with the ultrafast dynamics of 8′CA in ethanol[25] and 8′CA, 10′CA and 12′CA in an ethanol/tetrahydrofuran mixture.[26] In the former study, a time constant of 25 ps was deduced from the absorption decay at 530 nm after photoexcitation at 480 nm and ascribed to the lifetime of the S_1 state. In contrast to time-resolved experiments for apocarotenals,[7] no stimulated emission and therefore no evidence of ICT character was found at probe wavelengths in the near IR (850 nm).[25] In the latter study, time-resolved absorption spectra of 8′CA, 10′CA and 12′CA were recorded over the range 400–800 nm (for 8′CA also in the range 820–1020 nm).[26] The transient $S_1 \rightarrow S_n$ spectra of the three molecules in the visible range exhibited approximately a

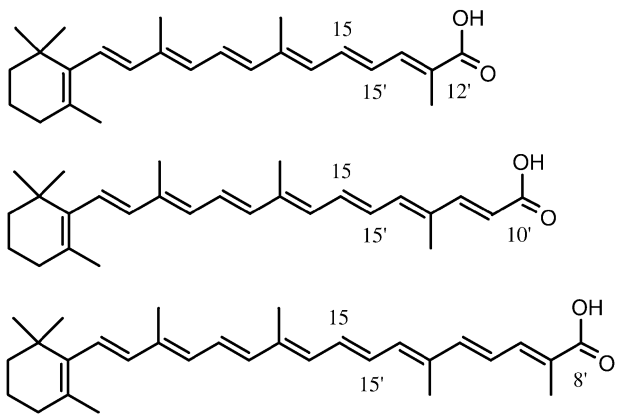

Fig. 1 Structures of 12′-apo-β-carotenoic-12′-acid, 10′-apo-β-carotenoic-10′-acid and 8′-apo-β-carotenoic-8′-acid (from top to bottom).

double band structure with features centered at 500/600 nm (12′CA), 520/620 nm (10′CA) and 540/640 nm (8′CA), where the amplitude of the higher wavelength band was always lower by a factor of 2–3. Both features decayed with the same time constant, and the dynamics for 12′CA and 10′CA were interpreted in terms of a simple three-state model $S_2(1^1B_u^+) \rightarrow S_1(2^1A_g^-) \rightarrow S_0(1^1A_g^-)$ (a possible involvement of an $^1B_u^-$-type intermediate state has been claimed in the case of 8′CA). In that study, no stimulated emission in the near IR was reported for 12′CA, 10′CA and 8′CA. Interpretation of the measurements is somewhat difficult, because the solvent polarity is unclear due to the fact that the ethanol/tetrahydrofuran mixing ratio was not specified. Our lifetimes reported below suggest, that a large excess of ethanol was likely present in these measurements.

Based on the experience from our earlier experiments on apocarotenoids we believe that ICT character is a fairly general property in the excited-state manifold of apocarotenoids with terminal carbonyl substitution. The motivation for our study was therefore twofold: First, we intended to find characteristic time-resolved stimulated emission features of 8′CA, 10′CA and 12′CA in the near IR range. These were indeed identified and assigned to the S_1/ICT state. Secondly, information on the solvent dependence of the S_1/ICT lifetime of carboxyl substituted apocarotenoids is obviously lacking, although such data are crucial for understanding the complex intramolecular dynamics in this class of molecules and related systems. Here, we present a first experimental investigation of these issues. The dynamics were monitored at several wavelengths covering the UV/Vis ground state bleaching ($S_0 \rightarrow S_2$), Vis excited state absorption (S_1/ICT $\rightarrow S_n$) and near IR excited state absorption/stimulated emission bands ($S_2 \rightarrow S_n$, S_1/ICT $\rightarrow S_0$) for a range of solvents covering a wide polarity range. In a future study we will provide time-resolved spectral data in the range 350−800 nm from PSCP spectroscopy, including a full global fitting of the ultrafast spectral dynamics.

2. Experimental

2.1 UV/Vis transient absorption experiments

The experimental setup was already described in our previous publications.[5,6] Briefly, the output of a Ti:sapphire oscillator-regenerative amplifier system (780 nm, 1 kHz, 1 mJ pulse^{-1}) was split up into two beams. One beam was frequency-doubled in a BBO crystal (λ_{pump} = 390 nm, $S_0 \rightarrow S_2$) and used for exciting the apocarotenoic acids into higher vibrational levels of the S_2 state. The other beam was either frequency-doubled in a BBO crystal (λ_{probe} = 390 nm) or directed into a home-built blue-pumped two-stage non-collinearly phase-matched optical parametric amplifier (NOPA) to generate the probe wavelength 575 nm (S_1/ICT $\rightarrow S_n$).[27–29] The NOPA output was subsequently compressed by a pair of quartz prisms.

A computer-controlled stage served to delay the pump and probe pulses with respect to each other. Each beam was then attenuated and mildly focused into the sample cell under a small angle (diameter of the light spot approximately 250 μm). The relative polarization of the pump and probe beams was

adjusted to 54.7° (magic angle) to avoid any contribution from orientational relaxation. Probe energies were measured by two photodiodes, which were located in front of and behind the flow quartz cuvette (1 mm path length), which contained the sample solution. A chopper wheel was used to block every second pump pulse. The change in optical density (ΔOD) was obtained from the differences of the optical densities with and without the pump beam. Typically, 4000–16 000 laser shots were averaged for each delay time. The time resolution of the setup was between 100 and 150 fs. Pulse energies for the pump and probe beams were kept at 2 μJ or less to ensure that nonlinear effects had no influence on the extracted time constants. This was also independently verified using another pump–probe setup, where pulse energies $\leq$0.4 μJ were used. The apocarotenoic acid concentration was typically between 2.5 and 7.5 $\times$ 10^{-5} M.

2.2 Near IR transient absorption/stimulated emission measurements

This setup has been used previously in our transient lens (TL) and transient absorption (TA) experiments.[13,30,31] Briefly, a mode-locked Ti:sapphire oscillator pumped by a Nd:YVO_4 laser was used to generate pulses at 850, 860 or 890 nm with a repetition rate of 82 MHz and an average laser power of about 1.0−1.5 W. A dichroic mirror was used to split the laser beam into two parts. One part passed through an acousto-optic modulator (AOM, operating at a frequency of 2 MHz provided by a pulse generator) and was subsequently frequency-doubled in a LBO crystal to generate an intensity-modulated pump beam (425, 430 or 445 nm) with pulse energies <0.1 nJ. The other part was used as probe beam, which had a typical energy <1 nJ $pulse^{-1}$ and was time-delayed with respect to the pump beam by means of a motorized delay line. The time resolution was typically about 120 fs. The pump and probe pulses were recombined in a collinear beam-in-beam arrangement, with the relative polarization set to magic angle to avoid any contributions from orientational relaxation. The pulses were mildly focused into a quartz flow-through cuvette containing the apocarotenoic acid solution and directed onto an avalanche photodiode. The time-dependent absorption/stimulated emission signal of the sample detected by the probe beam was fed into a lock-in amplifier which used the 2 MHz modulation of the pulse generator as its reference signal. The lock-in-signal was then transferred to a PC for further processing.

2.3 Chemicals

All-*trans* (all-*E*) samples of 8′-apo-β-carotenoic-8′-acid (8′CA), 10′-apo-β-carotenoic-10′-acid (10′CA), 12′-apo-β-carotenoic-12′-acid (12′CA), 8′-apo-β-caroten-8′-al, 12′-apo-β-caroten-12′-al and ethyl-8′-apo-β-caroten-8′-oate (–COOEt) were generously provided by BASF AG. All substances were used as received or purified by HPLC with final purities >97%. All solvents had a purity $\geq$99%. Steady-state absorption spectra were recorded on a Varian Cary 5E, fluorescence spectra on a Jobin-Yvon FluoroLog-3 spectrometer.

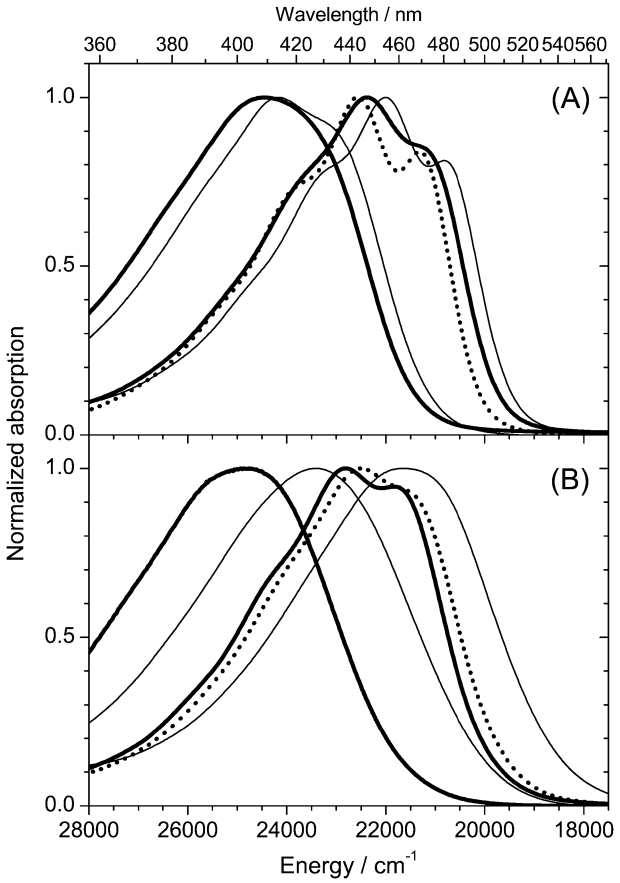

Fig. 2 Steady-state $S_0 \rightarrow S_2$ absorption spectra of apocarotenoids with different terminal carbonyl groups. (A) In *n*-hexane, from left to right: (thick solid line) 12′-apo-β-carotenoic-12′-acid; (thin solid line) 12′-apo-β-caroten-12′-al; (thick solid line) 8′-apo-β-carotenoic-8′-acid; (dotted line) ethyl-8′-apo-β-caroten-8′-oate; (thin solid line) 8′-apo-β-caroten-8′-al. (B) Same as (A) but in methanol.

3. Results and discussion

3.1 Steady-state absorption and fluorescence spectra of *n*′-apo-β-carotenoic-*n*′-acids

Fig. 2 compares $S_0 \rightarrow S_2$ steady-state absorption spectra of apocarotenoids with different terminal carbonyl groups in *n*-hexane (A) and methanol (B): 12′-apo-β-caroten-12′-al (12′C), 12′-apo-β-carotenoic-12′-acid (12′CA), 8′-apo-β-caroten-8′-al (8′C), 8′-apo-β-carotenoic-8′-acid (8′CA), and ethyl-8′-apo-β-caroten-8′-oate (8′CE). In Fig. 3, we present the absorption and fluorescence spectra of the three carboxylic acids 8′CA, 10′CA and 12′CA in *i*-octane and methanol, respectively. In the case of *nonpolar* solvents (Fig. 2(A)), changing from an aldehyde group to a carboxyl group results in a spectral shift to higher energy, both for 12′C/12′CA and 8′C/8′CA. Among the 8′-species, the aldehyde shows the strongest red-shift, *i.e.* the −CHO group exhibits the most efficient conjugation with the rest of the polyene chain. This is likely due to the following effects: (1) Larger residues, which are present in the other two species (8′CA and 8′CE) might favor structures where the carbonyl function is rotating out of the plane of the polyene system, minimizing steric congestion. (2) Differences in electronic structure induced by the different

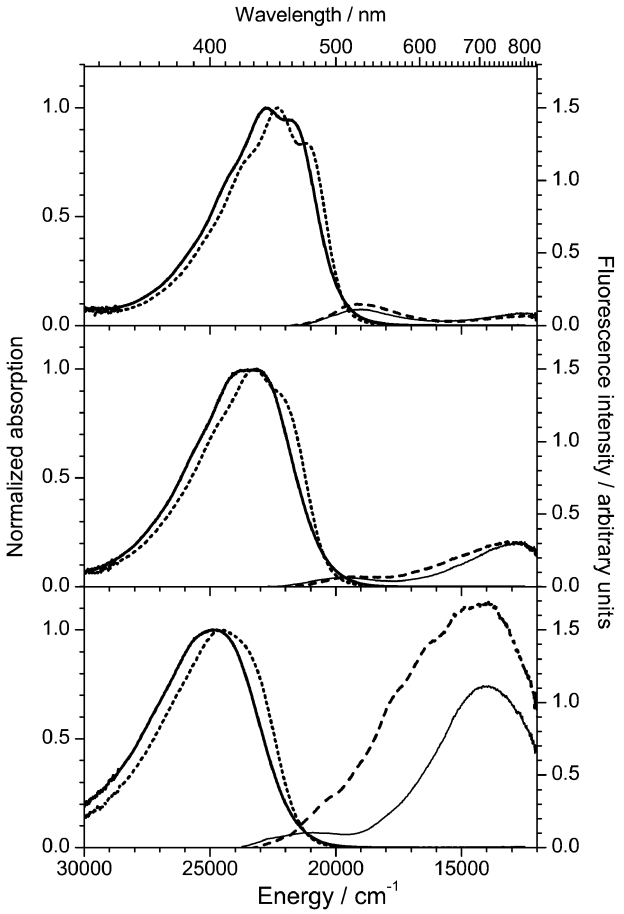

Fig. 3 Room-temperature absorption and fluorescence spectra of 8′-apo-β-carotenoic-8′-acid (8′CA, top), 10′-apo-β-carotenoic-10′-acid (10′CA, middle), and 12′-apo-β-carotenoic-12′-acid (12′CA, bottom). (Thick solid lines) absorption spectra in methanol; (dotted lines) absorption spectra in *i*-octane; (dashed lines) fluorescence spectra in *i*-octane (excitation wavelength: 447, 430 and 410 nm for 8′CA, 10′CA and 12′CA, respectively); (thin solid lines) fluorescence spectra in methanol (excitation wavelength: 440, 431 and 407 nm for 8′CA, 10′CA and 12′CA, respectively). The wavelength scale is shown on top as a reference. All absorption spectra are normalized to 1 (graduation on the left axis), whereas the fluorescence spectra show the measured relative amplitudes.

carbonyl functional groups will have an influence on the observed solvent shifts.

In *polar* solvents, the three carbonyl functional groups lead to different types of solvent-induced shifts relative to *n*-hexane. For example, the absorption spectra of the three acids shift to slightly *higher* energies in methanol (see Fig. 2(B) and the absorption maxima λ_{max} in Table 1). Therefore the acids behave similar to carotenoids without carbonyl substitution, where the position of the electronic absorption band correlates with the solvent polarizability (Lorentz–Lorenz function $R(n) = (n^2 - 1)/(n^2 + 2)$, n being the refractive index of the solvent).[13,32] In contrast, one observes a slight redshift of the absorption maximum in the case of an ester group (8′CE) and a pronounced red-shift of λ_{max} for the aldehydes 8′C and 12′C in methanol relative to that in *n*-hexane. Broadening of the vibronic structure in the absorption band was observed in methanol for all the species shown in Fig. 2. However, a complete loss of structure and an asymmetric broadening on the red side of the band was observed for the aldehyde only. These trends are not yet fully understood. In earlier investigations the asymmetric broadening observed for peridinin and apocarotenals in polar protic solvents was tentatively explained by the presence of different conformers absorbing at the red edge of the absorption spectrum.[7,11] If different conformers exist also for the acids, they obviously must have very similar absorption spectra. The increased broadening might be explained by a dipolar character of the electronic ground state S_0[8,11,21] and/or increased mixing of charge-transfer character into the S_2 state of extended polyene systems.[4,33]

In Fig. 3, the increasing red shift of the $S_0 \rightarrow S_2$ absorption spectrum with increasing conjugation length of the *n*′-apo-β-carotenoic-*n*′-acids is consistent with earlier studies on other carotenoids.[4,6,34] The smaller S_0-S_2 energy gap results from a stronger stabilization of the S_2 state relative to S_0. The reduction of the incremental shift on lengthening of the chain (*e.g.*, +24 nm for 12′CA → 10′CA and +15 nm for 10′CA → 8′CA in *i*-octane, Table 1) shows that the S_0-S_2 energy gap will converge toward a certain lower limit for polyenes with "infinitely" long conjugation. In all solvents one observes that the vibronic structure of the $S_0 \rightarrow S_2$ absorption band becomes more resolved upon extension of the conjugation, at least in the range studied here. Christensen *et al.* found a similar trend in their investigation of steady-state absorption spectra of seven apo-β-carotenes with different conjugation lengths ($N = 5-11$) in an ether/*i*-pentane/ethanol matrix at 77 K.[34] To explain this observation, a "distribution of conformers" model can be invoked: It is assumed that the non-planarity between the double bond in the β-ionone ring and the polyene backbone results in a smaller spread in transition energies for systems with increasingly longer conjugation. Optical excitation of longer carotenes would therefore select conformers with a less heterogeneous distribution of $S_0 \rightarrow S_2$ transition energies.

In addition, we recorded steady-state fluorescence spectra of the three apocarotenoic acids in *i*-octane (nonpolar) and methanol (polar). These are also included in Fig. 3. Beside the location of different emission bands they provide a comparison of the relative fluorescence amplitudes. The most prominent feature of the spectra in *i*-octane is the change from weak $S_2 \rightarrow S_0$ fluorescence around 530 nm (with possibly even weaker $S_1 \rightarrow S_0$ fluorescence around 800 nm) observed for 8′-apo-β-carotenoic-8′-acid to $S_1 \rightarrow S_0$ emission for 12′-apo-β-carotenoic-12′-acid peaking around 720 nm. For the 12′-species the $S_2 \rightarrow S_0$ fluorescence is probably buried under the blue edge of the $S_1 \rightarrow S_0$ main band, whereas the left part of the fluorescence spectrum of the 8′-species almost resembles the mirror image of the $S_0 \rightarrow S_2$ absorption spectrum. This behavior is consistent with that observed for other carotenoid series[34–39] where a relatively abrupt change in emission behavior occurs upon extension of the conjugated system. From comparison with other carotenoids the position of the $S_0 \rightarrow S_1(0-0)$ transition can be assigned to the shoulder appearing around 18 000 cm^{-1}. This is consistent with the value of 17 750 cm^{-1} previously deduced by us for the corresponding aldehyde 12′-apo-β-caroten-12′-al.[6] The crossover from $S_1 \rightarrow S_0$ to

Table 1 Lifetime τ_1 (S_1/ICT $\rightarrow$ S_0) of n'-apo-β-carotenoic-n'-acids (n = 8, 10, 12) in various solvents at 298 K

				λ_{max} (nm)[b]					τ_1 (ps)		
Solvent	$R(n)$[a]	$R(\varepsilon)$[a]	Δf[a]	12′CA	10′CA	8′CA	λ_{pump} (nm)	λ_{probe} (nm)	12′CA	10′CA	8′CA
n-hexane	0.23	0.23	0	408	432	447	390	390	233	67	22
							390	575	203	74	23
i-octane	0.24	0.24	0	411	—	—	430	860	203	—	—
Tetrahydrofuran	0.25	0.69	0.44	407	429	448	390	390	221	79	25
							390	575	222	78	25
							425	850	225	—	—
n-heptanol	0.26	0.78	0.53	411	—	—	425	850	203	—	—
n-butanol	0.24	0.85	0.61	409	—	—	425	850	164	—	—
Acetone	0.22	0.87	0.65	407	425	445	390	390	161	62	23
							390	575	157	66	25
							430	860	136	—	26
Excess ethanol/ tetrahydrofuran[c]	—	—	—	406	—	—	426	420–800	122	—	—
				—	435	—	445	420–800	—	64	—
				—	—	441	460	420–800	—	—	23
Ethanol	0.22	0.89	0.67	407	—	443	425	850	108	—	—
							430	860	111	—	29
						437[d]	480[d]	530[d]	—	—	25[d]
Acetonitrile	0.21	0.92	0.71	409	—	444	430	860	58	—	24
Methanol	0.20	0.91	0.71	406	429	441	390	390	56	34	22
							390	575	60	33	24
							430	860	49	—	25
							445	890	—	—	24

[a] $\Delta f = R(\varepsilon) - R(n)$, where $R(\varepsilon) = (\varepsilon - 1)/(\varepsilon + 2)$ and $R(n) = (n^2 - 1)/(n^2 + 2)$ with the dielectric constant ε and the index of refraction n of the solvent (ref. 42). [b] Position of the maximum of the $S_0 \rightarrow S_2$ absorption band. [c] All values from ref. 26: Steady-state absorption spectra in ethanol; time-resolved measurements were carried out in an ethanol/THF mixture with an unspecified excess of ethanol using a white-light continuum for probing. [d] From ref. 25: Additional measurements at λ_{probe} = 850 nm did not detect S_1/ICT $\rightarrow$ S_0 stimulated emission.

$S_2 \rightarrow S_0$ fluorescence with increasing conjugation length in nonpolar solvents can be explained by the decrease of the time constant τ_1 (*i.e.*, increase of the rate constant k_1) of $S_1 \rightarrow S_0$ internal conversion with decreasing S_1–S_0 energy gap (see below), which results in a lower quantum yield for $S_1 \rightarrow S_0$ fluorescence of 8′CA compared to 12′CA (provided that the radiative rate constants for the $S_1 \rightarrow S_0$ transition of the acids are comparable). 10′CA shows the expected "intermediate" behavior with a dominant but relatively weak $S_1 \rightarrow S_0$ emission (peak around 800 nm). Assuming not too different radiative rate constants for $S_2 \rightarrow S_0$ fluorescence of the three acids, the similar amplitudes of the $S_2 \rightarrow S_0$ fluorescence in the spectra is consistent with experimental observations that the $S_2 \rightarrow S_1$ internal conversion step of carotenoids is always very fast (on the order of 100–200 fs) and only weakly dependent on conjugation length.[1]

The fluorescence spectra in polar protic methanol look qualitatively similar to those in *i*-octane. The main difference is observed for the 12′-species where the $S_1 \rightarrow S_0$ emission in methanol has a less pronounced blue shoulder and no structure. The amplitude of the $S_1 \rightarrow S_0$ emission of 12′CA in methanol is smaller than in *i*-octane (ratio $\sim$2 : 3 at the band maximum), which is a bit surprising considering the roughly four times smaller lifetime of the lowest electronically excited state in methanol we report below. One reasonable explanation could be that the nature of the emissive state changes, such that its radiative rate constant becomes larger,[6] *e.g.* by acquiring more substantial intramolecular charge transfer character.[11,21,22] Such an interpretation is consistent with the strong stimulated emission observed in the transient pump–probe signals in the near IR region presented below. A simple estimate based on relative fluorescence intensities and lifetimes of the stimulated emission in *i*-octane and methanol suggest that the radiative rate constant increases by roughly a factor of 3 in the latter solvent.

3.2 Transient absorption signals

The measurements of time-resolved pump–probe signals for the three n'-apo-β-carotenoic-n'-acids (n = 8, 10, 12) were carried out in liquids at room temperature. Various solvents were chosen to cover a wide polarity range. Time constants τ_1 of the S_1/ICT $\rightarrow$ S_0 internal conversion process for all measurements are summarized in Table 1 in a systematic listing of conjugation length, solvent polarity and pump/probe wavelengths.

3.2.1 12′-Apo-β-carotenoic-12′-acid. Representative transient absorption signals for 12′-apo-β-carotenoic-12′-acid in tetrahydrofuran are shown in Fig. 4, where we plot the normalized ΔOD as a function of the pump–probe delay.

12′CA was excited to the S_2 state at 390 nm which is located to the blue of the absorption maximum of the $S_0 \rightarrow S_2$ transition. The subsequent dynamics were probed at the wavelengths 390 nm (ground state recovery, GSR) and 575 nm (excited state absorption, ESA). For 12′-apo-β-carotenoic-12′-acid, the GSR signals at the probe wavelength 390 nm show an immediate drop at $t = 0$. Subsequently, the negative signal decays back to zero on a slower timescale. The fast initial drop is due to up-pumping of 12′-apo-β-carotenoic-12′-acid to the S_2 state. After a very fast IC step $S_2 \rightarrow S_1$/ICT, which typically occurs with a time constant $\tau_2 = 100-200$ fs for most carotenoids,[1] the second IC step S_1/ICT $\rightarrow S_0$ takes place resulting in a slower final recovery of the absorption signal. The signal can be analyzed in the framework of a simple kinetic model assuming two consecutive IC processes $S_2 \rightarrow S_1$/ICT $\rightarrow S_0$, with characteristic time constants τ_2 ($=k_2^{-1}$) for the $S_2 \rightarrow S_1$/ICT and τ_1 ($=k_1^{-1}$) for the S_1/ICT $\rightarrow S_0$ steps (where k_2 and k_1 are the corresponding rate constants).[5] Using this model, one determines τ_1 to be 233 ps in *n*-hexane and 56 ps in methanol (Table 1), with estimated uncertainties of the time constants τ_1 of less than ten percent. All $S_0 \rightarrow S_2$ and S_1/ICT $\rightarrow S_n$ absorption-time profiles in this work were well-reproduced by this kinetic model with a typical regression coefficient of 0.9998. A Levenberg–Marquardt least squares fitting procedure was used to extract the best fit parameters for the time constants τ_1.

The probe wavelength 575 nm is located in the region of the ESA band S_1/ICT $\rightarrow S_n$ of 12′-apo-β-carotenoic-12′-acid.[26] Therefore the fast initial rise of the signal within the experimental time resolution is due to formation of S_1/ICT state population by excitation of the molecules to the S_2 state and subsequent ultrafast IC. On the basis of the current data we can only give a rough estimate for this step of $\tau_2 \leq 300$ fs. The ESA profiles decay with the time constants $\tau_1(S_1/\text{ICT} \rightarrow S_0) = 203$ and 60 ps for *n*-hexane and methanol, respectively. These values are in good agreement with those extracted from the GSR profiles recorded at 390 nm. Qualitatively similar to the case of 12′-apo-β-caroten-12′-al, the τ_1 values for 12′-apo-β-carotenoic-12′-acid show a pronounced dependence on the solvent polarity (see below).

Additional time-resolved absorption traces at 850, 860 or 890 nm have been obtained using a different setup at corresponding pump wavelengths of 425, 430 or 445 nm. Fig. 5 shows representative absorption/stimulated emission signals observed at 860 nm for 12′CA in *i*-octane and in methanol. A strong ultrafast initial spike is due to $S_2 \rightarrow S_n$ absorption, which is followed by formation of stimulated emission (SE). Such an SE feature was not reported in the previous studies of 12′CA.[25,26] We assign the SE to a low-lying electronic state with intramolecular charge transfer character (S_1/ICT $\rightarrow S_0$). The dynamics of 12′CA showed a strong dependence on the solvent environment. For instance, the transients decayed with time constants $\tau_1(S_1/\text{ICT} \rightarrow S_0) = 203$ and 49 ps for *i*-octane and methanol, respectively. These τ_1 values were obtained from simple monoexponential fits to the final well-separated decay of the SE. Except for THF, the lifetimes extracted from the SE decays are systematically shorter by $\sim 10\%$ than those extracted from the GSR (at 390 nm) and ESA (at 575 nm) profiles in nonpolar and polar solvents (see Table 1). We postpone a detailed global analysis of the traces to a future

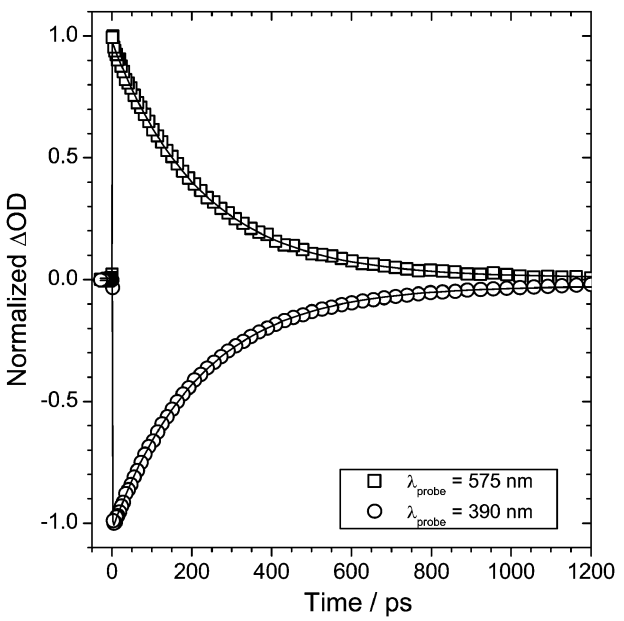

Fig. 4 Representative TA signals for 12′-apo-β-carotenoic-12′-acid in tetrahydrofuran after excitation to the S_2 state at 390 nm. Open squares: S_1/ICT $\rightarrow S_n$ absorption at 575 nm. Open circles: $S_0 \rightarrow S_2$ absorption at 390 nm. Solid lines are fits using the model from ref. 5. Time constants τ_1 for the S_1/ICT $\rightarrow S_0$ IC process can be found in Table 1.

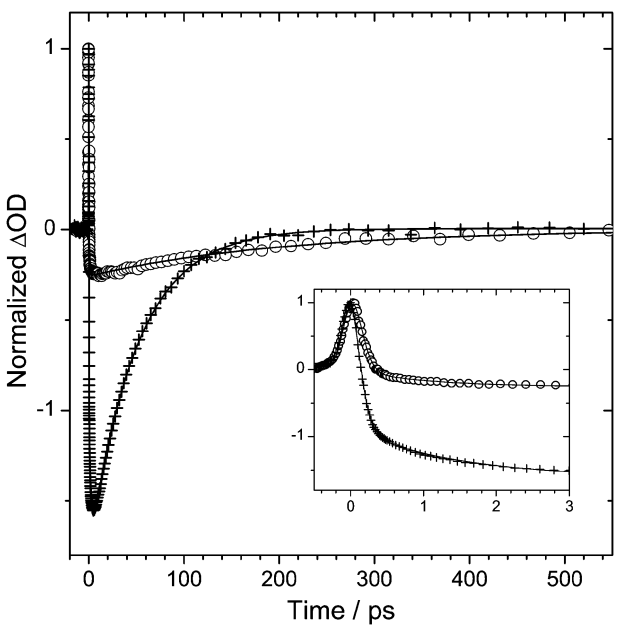

Fig. 5 Examples of time-resolved transient absorption/stimulated emission signals of 12′-apo-β-carotenoic-12′-acid in *i*-octane (○) and methanol (+). $\lambda_{pump} = 430$ nm and $\lambda_{probe} = 860$ nm. Signals are normalized to the maximum of the $S_2 \rightarrow S_n$ absorption. The evolution of the signals at early times is shown in the inset. Lines are intended only as a guide for the eye and have no further significance. τ_1 values obtained from a monoexponential fit to the final SE decay are summarized in Table 1.

publication, where we will present a refined model based on results from broadband absorption spectroscopy employing supercontinuum probing in the range 350–800 nm.

We also note that the SE feature exhibits a delayed appearance in all solvents (see the inset in Fig. 5), similar to our previous study of the corresponding apocarotenals[7] and earlier studies on peridinin.[10] Similarly, the ESA signals at 575 nm show an analogous weak "rise component". In the previous paper,[7] we proposed a simple model, which accounted for the observed dynamics: It features excited state branching from S_2 to populate separate S_1 and ICT states, which are connected by an equilibrium. Only the latter state emits in the near IR, and the delayed appearance of part of the SE is then due to formation of ICT population from the S_1 state. Correspondingly, the rise in the Vis region is due to formation of transient absorption from the ICT part. Preliminary fitting of the 12′CA transients provides solvent dependent time constants for this "delay" between 0.6–3.0 ps, which is in the same range as for the related aldehyde 12′-apo-β-caroten-12′-al (0.9–2.5 ps).[7] Broadband probing in combination with a global kinetic analysis will be required for an accurate analysis of this additional component and a complete deconvolution of the transient ESA band in the visible region.

The amplitude ratio of S_1/ICT $\rightarrow$ S_0 stimulated emission relative to S_2 $\rightarrow$ S_n absorption was smaller in nonpolar solvents than in polar solvents. Similar to our previous study of 12′-apo-β-caroten-12′-al and 8′-apo-β-caroten-8′-al, stimulated emission of 12′CA was observed in all solvents: strong in polar media and much weaker in nonpolar ones. The results indicate the involvement of intramolecular charge transfer (ICT) character in the excited state dynamics, regardless of solvent polarity.

3.2.2 10′-Apo-β-carotenoic-10′-acid. We have also obtained transient absorption signals for 10′CA in *n*-hexane, tetrahydrofuran, acetone and methanol (not shown here). The carotenoid was excited at 390 nm (blue edge of the S_0 $\rightarrow$ S_2 transition), and the subsequent dynamics were probed at the wavelengths 390 nm (GSR) and 575 nm (ESA). Time constants τ_1 are also summarized in Table 1. Upon 390 nm excitation of 10′CA in *n*-hexane and tetrahydrofuran, a variation of the time constants with probe wavelength was observed in the range τ_1 = 67–79 ps. In acetone, slightly smaller time constants (62–66 ps) were obtained. On the other hand, we observed an almost twice as fast decay kinetics of 10′CA in methanol (τ_1 = 33–34 ps).

3.2.3 8′-Apo-β-carotenoic-8′-acid. In the case of 8′CA, τ_1 was practically insensitive to the change of the excitation wavelength, probe wavelength and the solvent polarity (Table 1). All τ_1 values fall in the range 22–29 ps. It is interesting to compare these τ_1 values with previous measurements for 8′-apo-β-caroten-8′-al[6,7] and additional data sets from other groups,[4,40,41] where this species was excited at 490 or 510 nm, which is close to the 0–0 transition of the S_0 $\rightarrow$ S_2 band: He *et al.*[4,40] obtained τ_1 = 26.4 ps in 3-methylpentane after excitation at 490 nm (probed at 555 nm); similarly, Wasielewski *et al.* measured τ_1 = 25.1 ps in toluene for excitation at 510 nm (probed at 480 nm).[41] There appears to be no apparent influence of the excitation wavelength on the τ_1 values in the case of 8′-apo-β-caroten-8′-al. Within experimental error, the τ_1 values of 8′-apo-β-caroten-8′-al in nonpolar and mildly polar solvents are comparable to those of 8′CA. However, the aldehyde exhibits a pronounced reduction of τ_1 in polar environments, where *e.g.* τ_1 = 8.6 ps is obtained in methanol.[6]

In the near IR region at 860 and 890 nm, we also observed stimulated emission signals from 8′CA in acetone, ethanol, acetonitrile and methanol. They were much weaker than for 12′CA, possibly due to the shift of the emission maximum to longer wavelengths in the case of 8′CA. We note that τ_1 values obtained from the stimulated emission signals were almost identical to those measured in the S_0 $\rightarrow$ S_2 and S_1/ICT $\rightarrow$ S_n absorption bands (see Table 1). In this case, the SE in nonpolar solvents is too weak to be detected in this wavelength range.

3.3 Conjugation length and solvent dependence of the IC time constant τ_1

The GSR, ESA and SE profiles of the apocarotenoic acids are qualitatively similar. However, the IC time constant τ_1 for these three species decreases with increasing conjugation length, as shown in Table 1. For instance, τ_1 values are 222 ps, 78 ps and 25 ps, for 12′CA, 10′CA and 8′CA in tetrahydrofuran, respectively. This is a common feature in the excited state dynamics of carotenoids, see *e.g.* ref. 6 and 23.

Another interesting difference with respect to the τ_1 values of the three apocarotenoic acids was a marked change of the solvent polarity dependence when their conjugation length was shortened. The polarity can be quantified in terms of the solvent polarity factor Δf defined as

$$\Delta f = \frac{\varepsilon - 1}{\varepsilon + 2} - \frac{n^2 - 1}{n^2 + 2} \quad (1)$$

where values for the dielectric constant ε and index of refraction n were taken from the literature.[42] A pronounced decrease of τ_1 was observed in 12′CA for $\Delta f > 0.5$ ($\sim$218 ps in *n*-hexane and $\sim$55 ps in methanol). In the case of 10′CA, τ_1 values were insensitive to the polarity change in the range Δf = 0–0.6 ($\sim$75 ps), but a pronounced drop of τ_1 was observed in methanol (Δf = 0.71, τ_1 = 34 ps). For 8′CA, we did not observe any systematic change of τ_1 with solvent polarity over the range Δf = 0–0.7. Apparently, there are characteristic differences regarding the onset and the strength of the solvent dependence of τ_1 between the different apocarotenoic acids. Fig. 6 summarizes these findings.

Similar observations of different solvent polarity dependence of τ_1 for different conjugation lengths were made in the case of the *n*′-apo-β-caroten-*n*′-als (*n* = 4, 8, 12).[6,7] For instance, in the case of 12′-apo-β-caroten-12′-al, time-resolved transient absorption data recorded in the S_0 $\rightarrow$ S_2 and S_1/ICT $\rightarrow$ S_n absorption bands and pump–probe measurements in the near infrared region suggested that in the lower polarity range (Δf = 0–0.3) the τ_1 values are not particularly sensitive to the solvent polarity and are very similar to that of 12′CA. However, τ_1 values were almost linearly correlated with Δf over the range 0.3–0.7. While a qualitatively similar effect is also seen for 12′CA, the onset of solvent polarity dependence of τ_1

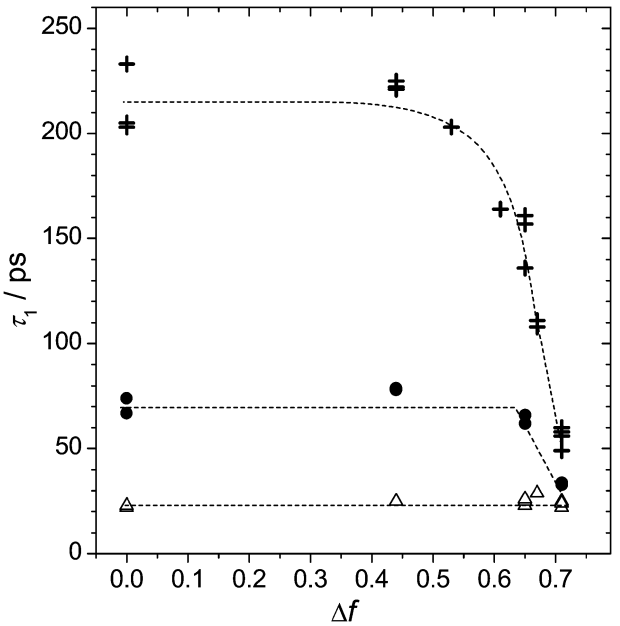

Fig. 6 Time constant τ_1 for the S_1/ICT → S_0 IC process of n'-apo-β-carotenoic-n'-acids as a function of solvent polarity: (+) 12′-apo-β-carotenoic-12′-acid; (●) 10′-apo-β-carotenoic-10′-acid; and (△) 8′-apo-β-carotenoic-8′-acid. For a summary of τ_1 values see Table 1. Dashed lines are intended only as a guide for the eye.

appears at a considerably higher Δf value (~0.5) compared to the aldehyde. For 8′-apo-β-caroten-8′-al, the τ_1 values decreased only at the highest Δf values, whereas for 8′CA such a decrease was not observed.

The reason for the different behavior regarding the onset and the strength of polarity dependence for apocarotenoic acids and apocarotenals is not yet clear, but can be probably rationalized in terms of the varying S_1/ICT–S_0 energy gap. Several effects might play a role: (1) Steric effects (worse conjugation for the bulky acid group) or (2) differences in the electronic properties of terminal –COOH and –CHO groups with respect to stabilizing charge separation, and therefore ICT formation, in the excited state. For larger conjugation lengths the S_1/ICT state might be already energetically so low that solvent dependent ICT stabilization has only a minor influence on the rate constant of internal conversion to S_0.

4. Conclusions

We have employed femtosecond pump–probe transient absorption spectroscopy to characterize the solvent dependence of the IC processes of a series of n'-apo-β-carotenoic-n'-acids (with n = 8, 10 and 12). 8′-Apo-β-carotenoic-8′-acid, having the largest number of conjugated double bonds, shows the smallest time constant (largest IC rate constant) for the S_1/ICT → S_0 transition, and in this case τ_1 is almost independent of solvent polarity (~24 ps). For the shorter 10′-apo-β-carotenoic-10′-acid a pronounced reduction of τ_1 from *ca.* 71 to 34 ps was observed when changing from *n*-hexane to methanol. This change is however still much weaker than for the even shorter 12′-apo-β-carotenoic-12′-acid (~218 and 55 ps, respectively). The conjugation length dependence of τ_1 in the nonpolar medium *n*-hexane can be qualitatively rationalized in terms of an energy gap law approach based on energy differences between the ground and first excited electronic state. The values are comparable with the corresponding 12′- and 8′-aldehydes studies previously in our groups.[5–7] In highly polar solvents like methanol the IC process is in all cases not as strongly accelerated as in the aldehydes.

For apocarotenoic acids with shorter conjugation length (and thus a long S_1 lifetime in nonpolar solvents), an "S_1/ICT" state is stabilized in highly polar solvents, which leads to the pronounced reduction of the lifetime. A characteristic signature of this state is its stimulated emission in the near IR. For apocarotenoic acids with longer conjugation length, the lifetime of the S_1 state is already short in nonpolar solvents, so the influence of ICT character on the lifetime appears to become less and less important with increasing conjugation length.

The differences between the 12′-species with terminal aldehyde and carboxyl groups are particularly interesting. In the latter case, the onset of the τ_1 polarity dependence appears at markedly higher Δf values, and is also less pronounced. Two effects could be responsible for such a behavior: The incremental stabilization of the ICT region of the "S_1/ICT" state with increasing polarity could be weaker for the acid than for the aldehyde. In addition, even for comparable incremental stabilization of the ICT part with increasing Δf for both types of substituents, the ICT region of 12′-apo-β-carotenoic-12′-acid in nonpolar solvents might be located higher above the S_1 part, so that it falls energetically below the S_1 part only at considerably larger Δf, consistent with the experimental observation of the shifted onset of the τ_1 decay. Clearly, at least some information on the energetic positions of the S_0 and "S_1/ICT" states (and thus the energy gap, which probably controls τ_1) will be required for further interpretation. We have therefore very recently launched quantum mechanical calculations for the electronically excited states of carbonyl substituted carotenoids. Together with ongoing pump–supercontinuum probe measurements in our group we plan to obtain a complete view of the excited state dynamics of low-lying electronic states of the apocarotenoic acids and related compounds.

Acknowledgements

Financial support by the German Science Foundation is gratefully acknowledged. We would like to thank J. Troe, J. Schroeder, and T. Polívka for stimulating discussions and S. Druzhinin for his advice during the steady-state fluorescence measurements. Special thanks go to the BASF AG, and here especially H. Ernst, for generously providing the all-*trans*-n'-apo-β-carotenoic-n'-acid samples and extensive support. Sample purification was performed by J. Bienert and J. Schimpfhauser.

References

1 T. Polívka and V. Sundström, *Chem. Rev.*, 2004, **104**, 2021.
2 E. Papagiannakis, M. Vengris, D. S. Larsen, I. H. M. van Stokkum, R. G. Hiller and R. van Grondelle, *J. Phys. Chem. B*, 2006, **110**, 512.

3 D. Zigmantas, R. G. Hiller, F. P. Sharples, H. A. Frank, V. Sundström and T. Polívka, *Phys. Chem. Chem. Phys.*, 2004, **6**, 3009.
4 Z. He, D. Gosztola, Y. Deng, G. Gao, M. R. Wasielewski and L. D. Kispert, *J. Phys. Chem. B*, 2000, **104**, 6668.
5 D. A. Wild, K. Winkler, S. Stalke, K. Oum and T. Lenzer, *Phys. Chem. Chem. Phys.*, 2006, **8**, 2499.
6 F. Ehlers, D. A. Wild, T. Lenzer and K. Oum, *J. Phys. Chem. A*, 2007, **111**, 2257.
7 M. Kopczynski, F. Ehlers, T. Lenzer and K. Oum, *J. Phys. Chem. A*, 2007, **111**, 5370.
8 H. A. Frank, J. A. Bautista, J. Josue, Z. Pendon, R. G. Hiller, F. P. Sharples, D. Gosztola and M. R. Wasielewski, *J. Phys. Chem. B*, 2000, **104**, 4569.
9 J. A. Bautista, R. E. Connors, B. B. Raju, R. G. Hiller, F. P. Sharples, D. Gosztola, M. R. Wasielewski and H. A. Frank, *J. Phys. Chem. A*, 1999, **103**, 8751.
10 D. Zigmantas, T. Polívka, R. G. Hiller, A. Yartsev and V. Sundström, *J. Phys. Chem. A*, 2001, **105**, 10296.
11 D. Zigmantas, R. G. Hiller, A. Yartsev, V. Sundström and T. Polívka, *J. Phys. Chem. B*, 2003, **107**, 5339.
12 P. Kukura, D. W. McCamant and R. A. Mathies, *J. Phys. Chem. A*, 2004, **108**, 5921.
13 M. Kopczynski, T. Lenzer, K. Oum, J. Seehusen, M. T. Seidel and V. G. Ushakov, *Phys. Chem. Chem. Phys.*, 2005, **7**, 2793.
14 D. Kosumi, M. Komukai, H. Hashimoto and M. Yoshizawa, *Phys. Rev. Lett.*, 2005, **95**, 213601.
15 G. Cerullo, D. Polli, G. Lanzani, S. De Silvestri, H. Hashimoto and R. J. Cogdell, *Science*, 2002, **298**, 2395.
16 T. Sashima, Y. Koyama, T. Yamada and H. Hashimoto, *J. Phys. Chem. B*, 2000, **104**, 5011.
17 J. L. P. Lustres, A. L. Dobryakov, A. Holzwarth and M. Veiga, *Angew. Chem., Int. Ed.*, 2007, **46**, 3758.
18 S. A. Kovalenko, A. L. Dobryakov, J. Ruthmann and N. P. Ernsting, *Phys. Rev. A: At., Mol., Opt. Phys.*, 1999, **59**, 2369.
19 J. L. P. Lustres, S. A. Kovalenko, M. Mosquera, T. Senyushkina, W. Flasche and N. P. Ernsting, *Angew. Chem., Int. Ed.*, 2005, **44**, 5635.
20 E. Papagiannakis, D. S. Larsen, I. H. M. van Stokkum, M. Vengris, R. G. Hiller and R. van Grondelle, *Biochemistry*, 2004, **43**, 15303.
21 S. Shima, R. P. Ilagan, N. Gillespie, B. J. Sommer, R. G. Hiller, F. P. Sharples, H. A. Frank and R. R. Birge, *J. Phys. Chem. A*, 2003, **107**, 8052.
22 H. M. Vaswani, C.-P. Hsu, M. Head-Gordon and G. R. Fleming, *J. Phys. Chem. B*, 2003, **107**, 7940.
23 H. A. Frank, V. Chynwat, R. Z. B. Desamero, R. Farhoosh, J. Erickson and J. Bautista, *Pure Appl. Chem.*, 1997, **69**, 2117.
24 V. Chynwat and H. A. Frank, *Chem. Phys.*, 1995, **194**, 237.
25 J. Pan, G. Benkö, Y. Xu, T. Pascher, L. Sun, V. Sundström and T. Polívka, *J. Am. Chem. Soc.*, 2002, **124**, 13949.
26 J. Xiang, F. S. Rondonuwu, Y. Kakitani, R. Fujii, Y. Watanabe, Y. Koyama, H. Nagae, Y. Yamano and M. Ito, *J. Phys. Chem. B*, 2005, **109**, 17066.
27 J. Piel, M. Beutter and E. Riedle, *Opt. Lett.*, 2000, **25**, 180.
28 E. Riedle, M. Beutter, S. Lochbrunner, J. Piel, S. Schenkl, S. Spörlein and W. Zinth, *Appl. Phys. B: Lasers Opt.*, 2000, **71**, 457.
29 T. Wilhelm, J. Piel and E. Riedle, *Opt. Lett.*, 1997, **22**, 1494.
30 T. Lenzer, K. Oum, J. Seehusen and M. T. Seidel, *J. Phys. Chem. A*, 2006, **110**, 3159.
31 R. Bürsing, T. Lenzer and K. Oum, *Chem. Phys.*, 2007, **331**, 403.
32 Z. Chen, C. Lee, T. Lenzer and K. Oum, *J. Phys. Chem. A*, 2006, **110**, 11291.
33 M. P. O'Neil, M. R. Wasielewski, M. M. Khaled and L. D. Kispert, *J. Chem. Phys.*, 1991, **95**, 7212.
34 R. L. Christensen, M. Goyette, L. Gallagher, J. Duncan, B. DeCoster, J. Lugtenburg, F. J. Jansen and I. van der Hoef, *J. Phys. Chem. A*, 1999, **103**, 2399.
35 S. A. Cosgrove, M. A. Guite, T. B. Burnell and R. L. Christensen, *J. Phys. Chem.*, 1990, **94**, 8118.
36 R. Snyder, E. Arvidson, C. Foote, L. Harrigan and R. L. Christensen, *J. Am. Chem. Soc.*, 1985, **107**, 4117.
37 B. DeCoster, R. L. Christensen, R. Gebhard, J. Lugtenburg, R. Farhoosh and H. A. Frank, *Biochem. Biophys. Acta*, 1992, **1102**, 107.
38 P. O. Andersson, S. M. Bachilo, R.-L. Chen and T. Gillbro, *J. Phys. Chem.*, 1995, **99**, 16199.
39 P. O. Andersson, T. Gillbro, A. E. Asato and R. S. H. Liu, *J. Lumin.*, 1992, **51**, 11.
40 Z. He, L. D. Kispert, R. M. Metzger, D. Gosztola and M. R. Wasielewski, *J. Phys. Chem. B*, 2000, **104**, 6302.
41 M. R. Wasielewski and L. D. Kispert, *Chem. Phys. Lett.*, 1986, **128**, 238.
42 *Handbook of Chemistry and Physics*, CRC Press, Boca Raton, 85th edn., 2004.

